OCEAN COLOR REMOTE SENSING USING POLARIZATION PROPERTIES OF REFLECTED SUNLIGHT

R. FROUIN[1], E. POULIQUEN[1], F.-M. BREON[2]

[1]: Scripps Institution of Oceanography,
La Jolla, California 92093-0221, USA

[2]: Laboratoire de Modélisation du Climat et de l'Environnement
CEA/DSM, 91191 Gif sur Yvette, France

ABSTRACT:

The effects of the atmosphere and surface on sunlight backscatterred to space by the ocean may be substantially reduced by using the unpolarized component of reflectance instead of total reflectance. At 450 nm, a wavelength of interest in ocean color remote sensing, and for typical conditions, 45% of the unpolarized reflectance may originate from the water body instead of 20% of the total reflectance, which represents a gain of a factor 2.2 in useful signal for water composition retrieval. The best viewing geometries are adjacent to the glitter region; they correspond to scattering angles around 100°, but they may change slightly depending on the polarization characteristics of the aerosols. As aerosol optical thickness increases, the atmosphere becomes less efficient at polarizing sunlight, and the enhancement of the water body contribution to unpolarized reflectance is reduced. Since the perturbing effects are smaller on unpolarized reflectance, at least for some viewing geometries, they may be more easily corrected, leading to a more accurate water-leaving signal and, therefore, more accurate estimates of phytoplankton pigment concentration.

KEY WORDS: Polarization, Ocean Color, Atmospheric Effects, Aerosols

1- INTRODUCTION

A major problem in ocean color remote sensing from space is the correction of top-of-atmosphere reflectance, the signal measured, for atmospheric and surface interference. At the wavelengths of interest, located in the blue-green region of the solar spectrum, as much as 90% of the photons reflected and/or backscattered to space may not have interacted with the water body and, thus, do not contain information on water composition. Since the perturbing effects are large, extraction of the useful signal requires accurate computation of those effects, which must be known to within a few percent to yield reasonably accurate estimates of phytoplankton pigment concentration. Uncertainties in radiometric calibration, aerosol characteristics, and sunglint and foam effects make the task arduous and, in some cases, impossible.

To reduce the influence of the atmosphere and surface on the top-of-atmosphere signal, one may exploit the polarization properties of reflected sunlight. Because molecules, aerosols, and hydrosols polarize sunlight differentially, there may be viewing geometries for which the contribution of the water body to the polarized or unpolarized components of total reflectance may be enhanced. Exploiting those properties would obviously require measurements of total reflectance and polarization rate. These measurements will be made by (or may be envisioned on) future sensors, such as the Polarization and Directionality of the Earth Reflectance (POLDER) imager (Deschamps et al., 1994). If the enhancement is substantial, correction of the perturbing effects becomes easier since accuracy constraints may not be as severe, leading to a more accurate water-leaving signal (the signal of interest).

Since the signal backscattered by the water body is polarized weakly after transmission accross the air-sea interface and through the atmosphere (see section 3), we focus our study on unpolarized reflectance. Using a Monte Carlo code we simulate the relative contribution of the water body to top-of-atmosphere unpolarized reflectance for varied conditions. We compare this contribution with that of the water body to total reflectance, identifying the viewing geometries that minimize atmospheric and surface effects. We quantify, for those geometries, the increase in the ratio of useful to total signal when using unpolarized reflectance instead of total reflectance.

2 - MODEL

To simulate the radiative transfer within the atmosphere, at the ocean surface, and within the ocean, we use a Monte Carlo model, an improved version of the model developed by Bréon (1992) to simulate the bidirectional reflectance of clouds. The improved version accounts for the polarization of scattered and reflected radiance.

The Monte Carlo model (hereafter referred to as MC) numerically simulates the path of photons interacting within the ocean-atmosphere system. The occurrence and type of interactions are determined by random numbers. In the atmosphere or in the water column, the pathlength L between two interactions is given by:

$$L = -\frac{1}{k_{ext}} \ln(\varepsilon)$$

where ε is a random number between 0 and 1 and k_{ext} is the extinction coefficient. Two angles are then necessary to define the new direction of motion: the scattering angle α (the angle between the two motion vectors before and after scattering), and the rotation angle ϕ (the angle between the scattering plane and a reference plane containing the motion vector before scattering). The angle a is obtained from the equation:

$$\int_0^{\alpha} P(\theta) \sin(\theta) d\theta = \varepsilon \int_0^{\pi} P(\theta) \sin(\theta) d\theta$$

and the angle ϕ is randomly chosen between 0 and 2π. In (2), $P(\theta)$ is the scattering phase function. It depends on the scattering element, either molecules, aerosols, or hydrosols.

At each scattering, the Stokes vector associated with a photon is modified according to (Chandrasekhar, 1960; Deirmendjian, 1969):

$$\begin{bmatrix} I_{=}' \\ I_{\perp}' \\ U' \\ V' \end{bmatrix} = \begin{vmatrix} P_1(\alpha) & & & \\ & P_2(\alpha) & & \\ & & P_3(\alpha) & -P_4(\alpha) \\ & & P_4(\alpha) & P_3(\alpha) \end{vmatrix} \begin{bmatrix} I_{=} \\ I_{\perp} \\ U \\ V \end{bmatrix}$$

When a photon reaches the surface (either from the atmosphere or from the ocean), the wave slope, β, is determined ramdomly according to wave slope statistics (Cox and Munk, 1954):

$$\tan(\beta) = \sigma[-\ln(\varepsilon)]^{\frac{1}{2}}$$

where s depends on the wind speed.

The photon is then either reflected or transmited through the interface. The Stokes vector associated to the photon becomes:

$$\begin{bmatrix} I_{=}' \\ I_{\perp}' \\ U' \\ V' \end{bmatrix} = \begin{vmatrix} r_{=}^2 & & & \\ & r_{\perp}^2 & & \\ & & -r_{=}r_{\perp} & \\ & & & -r_{=}r_{\perp} \end{vmatrix} \begin{bmatrix} I_{=} \\ I_{\perp} \\ U \\ V \end{bmatrix} \text{ or } \begin{bmatrix} I_{=}' \\ I_{\perp}' \\ U' \\ V' \end{bmatrix} = \begin{vmatrix} t_{=}^2 & & & \\ & t_{\perp}^2 & & \\ & & -t_{=}t_{\perp} & \\ & & & -t_{=}t_{\perp} \end{vmatrix} \begin{bmatrix} I_{=} \\ I_{\perp} \\ U \\ V \end{bmatrix}$$

where $r_{=}$, $r_{\perp}$, $t_{=}$, and $t_{\perp}$ depend on the incidence angle as in Takashima (1984).

The Stokes vector of all numerical "photons" reaching the top of the atmosphere within a given angular bin are summed. The four components of the vector yield the radiance, the polarization rate, and the direction of linear polarization.

We verified the model by comparing its output with that of another radiative transfer model that includes polarization, the doubling-adding model of Takashima (1984). Some of the comparison results are presented below. In the cases selected, the solar zenith angle is 30°, the surface wind speed is 5 ms-1, and the wavelength is 450 nm (molecular optical thickness of 0.22). The aerosol layer is located below the 800 mb level and its total optical thickness is 0.25. The aerosols have the size distribution and refractive index of the "Water Soluble" model of the World Meteorological Organization (WMO) (WCP, 1986). The effect of the water body is simplified by assuming that 2% of the irradiance penetrating the water is reflected isotropically as unpolarized radiance.

The reflectance (radiance normalized by the incident solar irradiance) and polarization rate in the principal plane, as estimated by both models, is presented in Fig. 1. The polarization rate is defined as the ratio of polarized reflectance and total reflectance. Solid circles denote the MC results, and open circles denote the doubling-adding results. The specular direction is on the right side of the figure, as indicated by the local maximum in reflectance when the viewing zenith angle is close to the solar zenith angle (Fig. 1, top). Since the MC values are representative of an angular bin, they are indicated at the bin center. On the other hand, the doubling-adding method computes the radiative transfer equations at precise angles. Note that the angular precision close to the limb is much better for the latter.

The two radiative transfer models validate each other in these comparisons. In Fig. 1, top, both models show a large reflectance increase near the limb as viewing zenith angle increases, which results from more important atmospheric scattering. They also show a similar glitter effect, whose amplitude and extension depends on wind speed (through the wave slope distribution). In Fig. 1, bottom, the maximum polarization rate, located around 50° viewing zenith angle, results from the combined effect of specular reflection (maximum polarization at the Brewster angle) and molecular scattering (maximum polarization at 90° scattering angle). As expected, the minimum polarization rate is found close to backscattering.

3 - RESULTS

For the purpose of our study, the MC simulations are performed at the wavelength of 450 nm, where phytoplankton absorb a substantial amount of light. The solar zenith angle is fixed at 30° and the wind speed at 5 ms^{-1}. The aerosols are represented by the "oceanic" and "water soluble" models of the WMO (WCP, 1986). They are located below 800 mb and their optical thickness is 0.2, a typical value for clear atmospheres. The hydrosols are phytoplankton particles. Their characteristics (size distribution, refractive index) are specified according to Zaneveld et al. (1974) and Aas (1981). Their volume number concentration, 1.19 10^{14} m^{-3}, is constant throughout the water column (homogeneous ocean) and corresponds to a pigment concentration (i.e., chlorophyll-*a*) of about 0.1 mgm^{-3}. In Table 1, the characteristics of the aerosols and hydrosols are summarized, and in Fig. 2 the respective scattering phase functions are displayed. The polarization rates for single scattering are not shown, but they do not exceed 0.5 (compared to the maximum value of almost 1 for molecules).

In Fig. 3, the total reflectance and the polarization rate of the ocean-atmosphere system is presented as a function of viewing geometry. The atmosphere contains "oceanic" aerosols. A basic feature is the large bidirectionality of the total reflectance (Fig. 3, top). Specular reflection results in higher reflectance values (0.25) around 30° viewing zenith angle and 180° relative azimuth angle. At high viewing zenith angles, the total reflectance reaches values of about 30%. Minimum values (0.1-0.12) are found outside the glitter region at viewing zenith angles below 60°. The polarization rate also exhibits large angular variability (Fig. 3, bottom). The maximum polarization rate (about 70%) is obtained at 50° viewing zenith angle in the principal plane ("forward" scattering), not at the Brewster angle nor at 60° viewing zenith angle, which would be expected in the case of only specular reflection or molecular scattering, respectively. The mimimum polarization rates are obtained at large scattering angles, around the direction of the sun in bakscattering.

Fig. 4 displays the top-of-atmosphere reflectance and the polarization rate of photons that have interacted with the water body. Reflectance values are small, not exceeding 0.03-0.04, and the

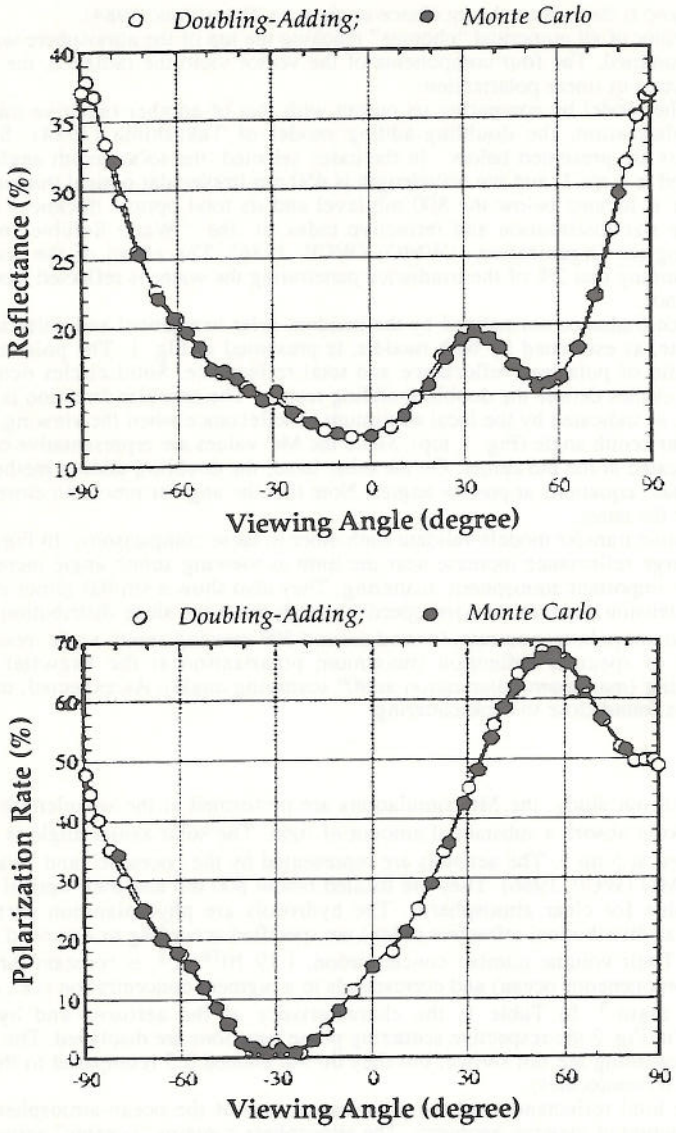

Fig. 1: Reflectance and polarization rate in the principal plane computed with the Monte Carlo code (solid circles) and with the doubling-adding code of Takashima (1984) (open circles). Sun zenith angle is 30°, wind speed is 5 ms^{-1}, and wavelength is 450 nm. Aerosols are of "water soluble" type; they are located below 800 mb and have an optical thickness of 0.25. The water body is Lambertian, with a reflectance of 2%.

Table 1. Optical characteristics of the scatterers at 450 nm.

Type	$dN(r)/dr$	r_{min} (μm)	r_{max} (μm)	m	σ_s (μm^2)	ω_o
Aerosols						
Oceanic	Log-normal	0.001	100	$1.38 - 5\ 10^{-9}i$	$0.36\ 10^{-1}$	1.00
Water Soluble	Log-normal	0.001	100	$1.53 - 5\ 10^{-3}i$	$0.68\ 10^{-1}$	0.93
Hydrosols	Junge	1.0	100	$1.38 - 5\ 10^{-3}i$	$0.60\ 10^{-1}$	0.89

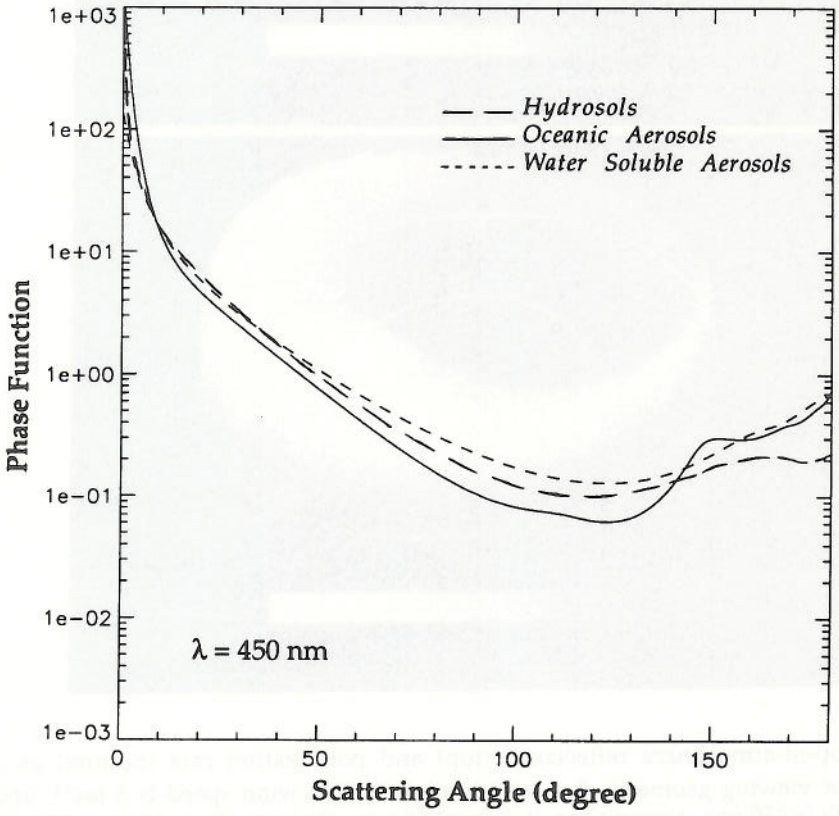

Fig. 2: Phase functions of the aerosols and hydrosols.

$\theta_s = 30^o$; $W = 5\ ms^{-1}$; *"Oceanic" Aerosols;* $\tau_{aer} = 0.2$; $C_{phy} = 0.1\ mgm^{-3}$

-all photons-

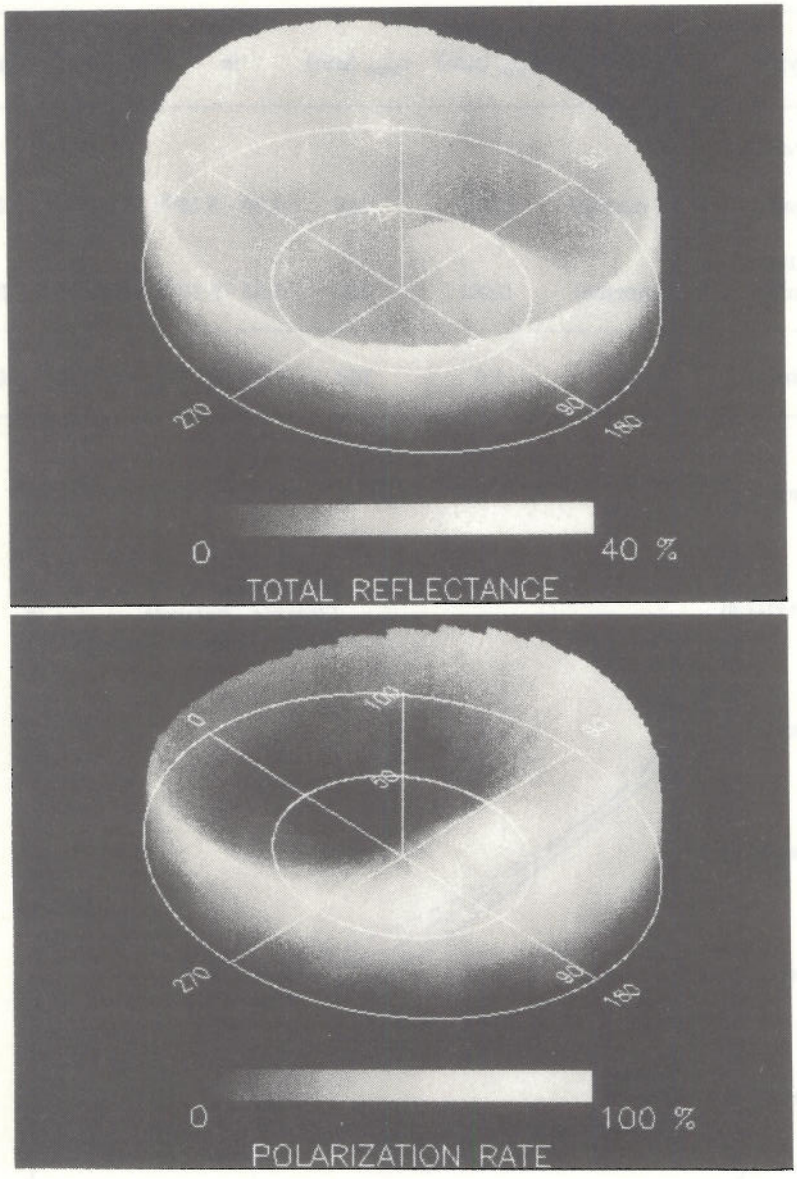

Fig. 3: Top-of-atmosphere reflectance (top) and polarization rate (bottom) as a function of viewing geometry. Sun zenith angle is 30°, wind speed is 5 ms^{-1}, and wavelength is 450 nm. Aerosols are of "oceanic " type; they are located below 800 mb and their optical thickness is 0.2. Hydrosols are phytoplankton particles; they are uniformly distributed vertically and their volume concentration number is 1.19 10^{14} m^{-3} (about 0.1 mgm^{-3}).

$\theta_s = 30^o$; $W = 5\ ms^{-1}$; *"Oceanic" Aerosols;* $\tau_{aer} = 0.2$; $C_{phy} = 0.1\ mgm^{-3}$
-photons that have interacted with the water body-

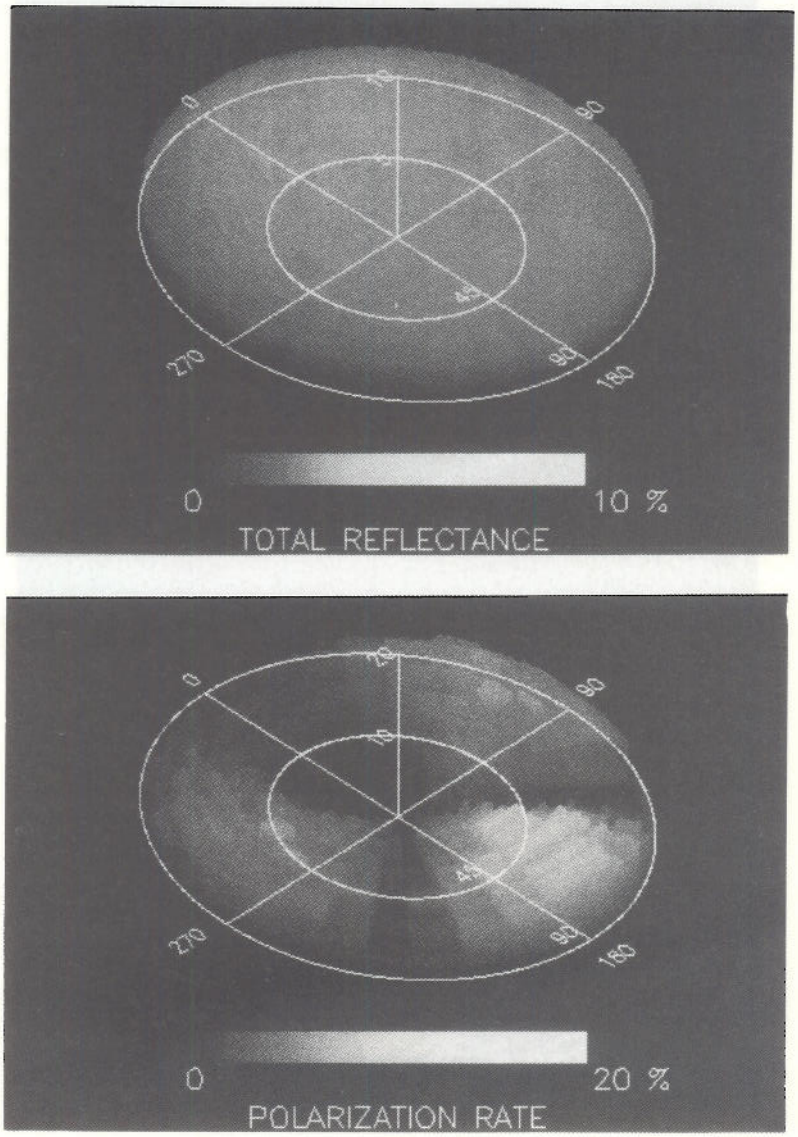

Fig. 4: Same as Fig. 3, but the contribution of photons that have interacted with the water body. Reflectance values are small (a few percent), and the signal is weakly polarized. Bidirectionality of the reflectance is practically negligible.

$W = 5\ ms^{-1}$; "Oceanic" Aerosols; $\tau_{aer} = 0.2$

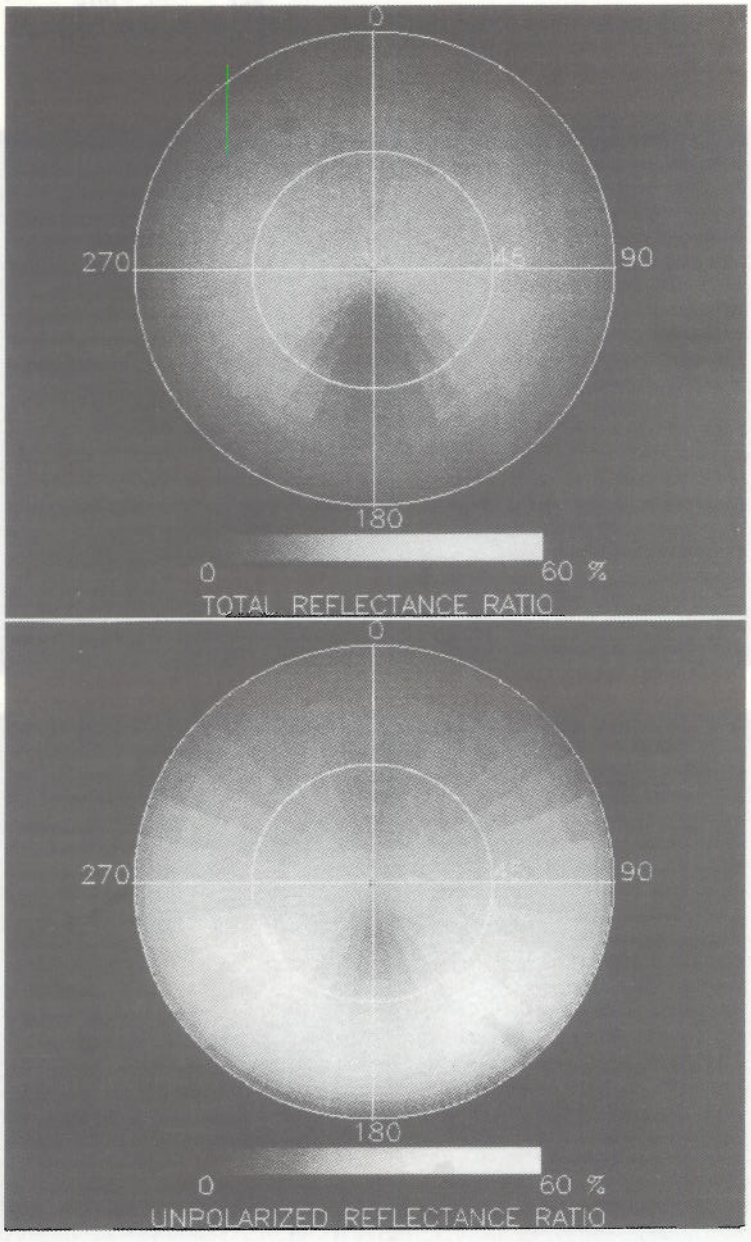

Fig. 5: (Top) Relative contribution to the top-of-atmosphere total reflectance of photons that have interacted with the water body; (Bottom) Same as (Top), but unpolarized reflectance. Atmospheric and oceanic conditions and sun geometry are those of Fig. 3. For some viewing geometries, outside the glitter region in forward scattering, the signal originating from the water body represents as much as 45% of the top-of-atmosphere unpolarized reflectance.

signal lacks directionality (Fig. 4, top). The polarization rate is also small irrespective of the viewing geometry, with maximum values of about 5% (Fig. 4, bottom). This suggests that it may not be appropriate to work with the polarized component of reflectance to enhance the relative contribution of the water body. As the ocean signal is weak and almost unpolarized, one may not want to deal with a noisy polarized signal, even though there are backscattering geometries for which the atmospheric and surface effects on the top-of-atmosphere polarized reflectance are practically eliminated (see Fig. 3, bottom).

The polar diagrams in Fig. 5 show the relative contribution to total and unpolarized reflectance of photons that have interacted with the water body. The characteristics of the ocean, atmosphere, and surface are the same as those of Figs. 3 and 4. Working with total reflectance (Fig. 5, top), the contribution of the water body does not exceed 20%. The highest values are obtained outside the glitter region for viewing zenith angles of less than 60°. For those geometries, the aerosol phase function is small. Apart from the glitter region, where values are obviously small, the minimum values are found at high viewing zenith angles, where atmospheric scattering dominates. Working with the unpolarized component of reflectance, by contrast (Fig. 5, bottom), the contribution of the water body reaches 45%, which represents a gain in useful signal of a factor of 2.2. The best viewing geometries are adjacent to the glitter region, at viewing zenith angles of about 50° (scattering angles of 100° or so). At these angles, polarization by air molecules and aerosols (combined) is maximum. As the relative azimuth angle decreases from 150°, the scattering angle decreases, making generally the air molecules and aerosols less efficient at polarizing sunlight. The result is a decreased contribution of the water boby (Fig. 5, bottom).

4- DISCUSSION

As shown above, using the unpolarized component of reflectance instead of total reflectance enhances, for some viewing geometries, the relative contribution of the water body to the signal measured at the top of the atmosphere. The gain obtained at 450 nm (a factor of 2) is substantial, making it easier to correct the top-of-atmosphere signal for atmospheric and surface effects (45% instead of 20% of the measured signal may now originate from the water body) and, therefore, to retrieve the signal backscattered by the water body. In fact, even in backscattering, at high viewing zenith angles, or in the glitter region, the unpolarized reflectance at the top of the atmosphere is generally less influenced by atmospheric and surface effects than the total reflectance (see Fig. 5). The results, though preliminary, strongly suggest that polarization is a useful property of light to improve ocean color remote sensing from space.

Since aerosols polarize incident sunlight less than molecules, the enhancement obtained using unpolarized reflectance is reduced as aerosol optical thickness is higher, all the more as multiple scattering, being mor efficient, further contributes to reduce polarization rate. When the aerosol optical thickness is 1, for instance, there is practically no gain in the relative contribution of the water body. Such conditions, however, are extreme, and not suitable for ocean color remote sensing.

Another point should be mentioned about aerosols. Mie calculations show distinct polarization signatures depending on type. The favorable viewing geometries, therefore, may be type-dependent. In general, however, the maximum polarization rates are found between scattering angles of 80° and 150°, which determines somewhat the potentially favorable geometries. In fact, simulations with "water-soluble" aerosols (not shown here) have revealed significant changes in the diagram of Fig. 5, bottom (e.g., a narrower range of favorable viewing geometries), but only a slight displacement of the location of the maximum values toward lower vewing zenith angles (higher scattering angles).

Depending on the surface conditions (e.g., wind speed), the glitter pattern may extend over a wider range of viewing angles, displacing the favorable geometries further off the principal plane. As solar zenith angle increases, those geometries become closer to nadir.

Using unpolarized reflectance, one may wonder about the sensitivity of the unpolarized signal backscattered by the water body (obtained after atmospheric corrections) to water composition and, in particular, phytoplankton pigment concentration. In the favorable geometry regions of Fig. 5, bottom, the water body exhibits polarization rates of about 20% with only 0.1 mgm^{-3} of pigments, the values obviously decreasing with increasing pigment concentration. These relatively low polarization rates suggest a sensitivity of the unpolarized signal to pigment concentration similar to that of the total signal, but slightly reduced since the polarization rate decreases when pigment concentration increases.

Looking to the future, starting in 1996 the POLDER instrument will measure the angular polarization properties of reflected sunlight. Although not all the spectral bands useful to ocean color remote sensing will have polarization capabilities, the data will provide the opportunity to test and verify many of the concepts and theoretical findings discussed above.

5- ACKNOWLEDGMENTS

This work has been supported by the National Aeronautics and Space Administration under grants NAGW-2774 (to R. Frouin) and NAGW-3498 (to R. Frouin), by the Centre National d'Etudes Spatiales, and by the California Space Institute. The helpful comments of and discussions with Drs. B. Bonnel, P.-Y. Deschamps, and Prof. M. Herman of the University of Lille, France, Dr. G. Mitchell from the Scripps Institution of Oceanography, and Prof. K. Voss of the University of Miami are gratefully acknowledged, as well as the programming assistance of Mr. J. McPherson of the Scripps Institution of Oceanography.

6- REFERENCES

Aas, E., 1981: The refractive index of phytoplankton. Institute Report Series No 46, Institut for Geophysikk, Oslo University.

Bréon, F.M.; 1992: Reflectance of Broken Cloud Fields: Simulation and Parameterization. *J. Atm. Sci.*, 49, 1221-1232.

Chandrasekhar, S., 1960: Radiative Transfer. Dover Publication, New York, 393 pp.

Cox, C., and W. Munk, 1954: Measurements of the Roughness of the Sea Surface from Photographs of the Sun's Glitter. *J. Opt. Soc. Amer.*, 44, 838, 850.Deirmendjian, D.; 1969: Electromagnetic scattering on Spherical Polydispersions. Elsevier, 290 pp.

Deschamps, P.-Y., F.-M. Bréon, M. Herman, M. Leroy, A. Podaire, A. Bricaud, J. C. Buriez, J.-L. Deuzé, and G. Sèze, 1994: The POLDER mission: instrument characteristics and scientific objectives. IEEE *Trans. Geo. Rem. Sen.*, in press.

Deschamps, P.-Y., and M. Viollier, 1987: Algorithm for ocean color from space and applications to CZCS data. *Adv. Space Res.*, 7, 11-19.

Takashima, T; 1984: Polarization effect on radiative transfer in planetary composite atmospheres with interacting interface. *Earth, Moon, and Planets*, 33, 59-97.

WCP, 1986: A preliminary cloudless standard atmosphere for radiation computation. WMO report No 24, Geneva.

Zaneveld, J. R., D. M. Roach, and H. Pak, 1974: The determination of the index of refraction of oceanic particulates. *J. Geophys. Res.*, 79, 4091-4095.